Bioorganic Chemistry 108 (2021) 104563

Contents lists available at ScienceDirect

Bioorganic Chemistry

journal homepage: www.elsevier.com/locate/bioorg

Investigation of pyrazolo[1,5-*a*]quinoxalin-4-ones as novel monoamine oxidase inhibitors

Valeria A. Panova [a], Sergey I. Filimonov [b], Zhanna V. Chirkova [b], Mariya V. Kabanova [b], Anton A. Shetnev [a], Mikhail K. Korsakov [a], Anél Petzer [c], Jacobus P. Petzer [c,*], Kyrill Yu Suponitsky [d,e]

[a] *Pharmaceutical Technology Transfer Center, Yaroslavl State Pedagogical University named after K.D. Ushinsky, 108 Respublikanskaya St., Yaroslavl, Russian Federation*
[b] *Yaroslavl State Technical University, 88 Moskovskii av., Yaroslavl, Russian Federation*
[c] *Pharmaceutical Chemistry and Centre of Excellence for Pharmaceutical Sciences, North-West University, Potchefstroom 2520, South Africa*
[d] *A.N. Nesmeyanov Institute of Organoelement Compounds, Russian Academy of Sciences, Vavilov St. 28, Moscow 119991, Russian Federation*
[e] *G.V. Plekhanov Russian University of Economics, Stremyanny per. 36, Moscow 117997, Russian Federation*

ARTICLE INFO

Keywords:
Monoamine oxidase
Inhibition
Selectivity
Depression
Parkinson's disease
Pyrazolo[1,5-*a*]quinoxalin-4-one

ABSTRACT

The monoamine oxidase (MAO) enzymes are key metabolic enzymes of neurotransmitter and other bioactive amines, and represent important drug targets for the treatment of neuropsychiatric and neurodegenerative disorders. Inhibitors of MAO are established medications for the treatment of depression and Parkinson's disease, and may have future roles in other disease states such as the therapy of prostate cancer, cardiovascular disease and inflammatory diseases. Based on these considerations, the present study synthesizes a series of 22 pyrazolo[1,5-*a*]quinoxalin-4-one derivatives and evaluated them as potential inhibitors of human MAO-A and MAO-B. The results show that 8 derivatives inhibit MAO-A, and 3 derivatives inhibit MAO-B with IC_{50} values in the submicromolar range (<1 μM). The most potent MAO-A inhibitor, N-[5-(acetyloxy)-2-(4-chlorophenyl)-4-oxo-4,5-dihydropyrazolo[1,5-*a*]quinoxalin-7-yl]acetamide (**7c**), exhibit an IC_{50} value of 0.028 μM and displays 50-fold selectivity for MAO-A over MAO-B. The most potent MAO-B inhibitor, 2-(4-methylphenyl)-4-oxo-4,5-dihydropyrazolo[1,5-*a*]quinoxaline-7-carbonitrile (**4f**), exhibit an IC_{50} value of 0.617 μM and displays 8-fold selectivity for MAO-B. This is the first report of MAO inhibition by pyrazolo[1,5-*a*]quinoxalin-4-one derivatives, and this study concludes that these compounds are suitable leads for the future development of MAO inhibitors, particularly of the MAO-A isoform.

1. Introduction

The monoamine oxidases (MAOs, EC 1.4.3.4) are flavin adenine dinucleotide (FAD) containing enzymes that are bound the outer membranes of mitochondria [1]. The MAOs catalyze the oxidation of various neurotransmitters and dietary amines to yield the corresponding imine intermediates, which are subsequently hydrolyzed to form an aldehyde and ammonia (or a substituted amine) (Fig. 1). Reoxidation of the FAD occurs with molecular oxygen to yield hydrogen peroxide as byproduct [1]. The two MAO isoforms, MAO-A and MAO-B, are approximately 70% similar on the amino acid sequence level, and are products of distinct genes [2,3]. Although the MAOs are expressed in the peripheral tissues and brain, certain tissues display specific expression of one of the isoforms. For example, MAO-A is found in the placenta and gastrointestinal tract, while human platelets and lymphocytes express only MAO-B [4,5].

Since the architectures and residues of the active sites of MAO-A and MAO-B are similar, considerable overlap in the substrate and inhibitor specificities occur between the two isoforms [6,7]. In this respect dopamine, adrenaline, noradrenaline and tyramine are substrates for both isoforms [8]. In contrast, serotonin is a MAO-A specific substrate while benzylamine and 2-phenylethylamine are specific substrates for

* Corresponding author.
E-mail addresses: v.panova@yspu.org (V.A. Panova), filimonovsi@ystu.ru (S.I. Filimonov), chirkovazhv@ystu.ru (Z.V. Chirkova), mariya_vk02@mail.ru (M.V. Kabanova), a.shetnev@yspu.org (A.A. Shetnev), mkkors@mail.ru (M.K. Korsakov), 12264954@nwu.ac.za (A. Petzer), jacques.petzer@nwu.ac.za (J.P. Petzer), kirshik@yahoo.com (K.Y. Suponitsky).

https://doi.org/10.1016/j.bioorg.2020.104563
Received 2 July 2020; Received in revised form 7 December 2020; Accepted 13 December 2020
Available online 15 December 2020

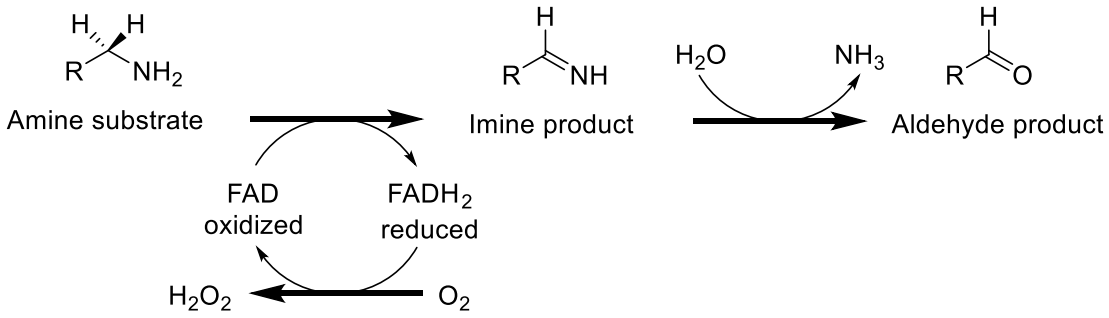

Fig. 1. The reaction catalyzed by MAO.

MAO-B. Based on their roles in the metabolism of neurotransmitters, the MAOs represent important drug targets for the treatment of neuropsychiatric and neurodegenerative disorders. Inhibitors of MAO are established medications for the treatment of depression and Parkinson's disease [8,9], and may have future roles in other disease states, most notably the therapy of prostate cancer, cardiovascular disease and inflammatory diseases [10–12]. In depression, MAO-A inhibitors act by blocking the central breakdown of serotonin and noradrenaline, while MAO-B inhibitors extend the central action of dopamine in Parkinson's disease, and are combined with levodopa for the treatment of motor fluctuations in Parkinson's disease [13,14]. Literature further reports that MAO inhibitors such as phenelzine and tranylcypromine lead to disease remission in patients suffering from Crohn's disease or rheumatoid arthritis [15,16]. While many of the therapeutic benefits of MAO inhibition are dependent on reducing the metabolic breakdown of neurotransmitters, hydrogen peroxide formed in the MAO catalytic cycle may contribute to the pathophysiology of certain disorders [17]. For example, it has been proposed that hydrogen peroxide produced by MAO may lead to oxidative damage to susceptible neurons in the brain, and thereby may contribute to neurodegeneration in Parkinson's disease [1]. Similarly MAO-A is a source of hydrogen peroxide in the heart which may lead to the development of heart disease through the intracellular production of reactive oxygen species [18,19]. By reducing the hydrogen peroxide production, isoform-selective MAO inhibitors may potentially protect against the development and progression of these diseases.

While certain inhibitors do not display isoform specificity (e.g. phenelzine, tranylcypromine), a number of reversible and irreversible inhibitors have been developed as specific inhibitors of either MAO-A or MAO-B [8,20]. For MAO-A, these include clorgyline, moclobemide and toloxatone, while selegiline, rasagiline and safinamide are specific MAO-B inhibitors. A number of MAO inhibitors are in clinical use as antidepressant and anxiolytic agents, and as treatments for Parkinson's disease. Based on the clinical and academic interest in MAO inhibitors, several research programs are underway to discover and develop MAO inhibitors [12]. In this respect, the current study synthesized a series of 22 pyrazolo[1,5-*a*]quinoxalin-4-one derivatives (Table 1) and evaluated them as potential inhibitors of human MAO-A and MAO-B. These compounds are novel and to the best of our knowledge this class of compounds has not yet been investigated as potential MAO inhibitors. Nor do the structures of the study compounds closely resemble known MAO inhibitors. It may, however, be noted that compounds with tricyclic fused ring systems have been reported to inhibit the MAOs, as exemplified with the MAO-A selective inhibitor, harmine [6]. The aim of this study was thus to discover novel compounds that may serve as leads for the future development of MAO inhibitors. Since this is the first investigation of the MAO inhibition properties of pyrazolo[1,5-*a*]quinoxalin-4-ones, this study may be viewed as an exploratory study and no attempt has been made to rationally select substituents R^1–R^3 (Table 1). Based on the results, future structure modifications will be guided by a more rational strategy (e.g. molecular docking) in an attempt to improve activity and properties.

2. Results and discussion

2.1. Chemistry

Previously, a two-stage selective method for the synthesis of 5-hydroxypyrazolo[1,5-*a*]quinoxalin-4-ones (**5**) from ethyl 3-arylpyrazole-5-carboxylates (**1**) and activated o-chloronitroarene (**2**) substrates has been developed (Fig. 2) [21]. The yields of these compounds were as high as 66%. The physical and chemical properties of the hydroxy group of the hydroxypyrazolo[1,5-*a*]quinoxalin-4-ones were similar to those of 1-hydroxyindoles. While being weakly soluble in most organic solvents, in the presence of base, compounds **5** (as the hydroxamic acids) dissolved in water due to the formation of the corresponding salt forms [22].

We have also developed and reported a catalytic method that selectively produces pyrazolo[1,5-*a*]quinoxalin-4-ones **4a**–**c** with yields as high as 73% using Pd/C (10%) as catalyst (method A). However, this method yielded poor results when the synthesis of derivatives containing cyano groups was attempted [23,24]. Therefore, an alternative method was developed which involved the *N*-dehydroxylation of the 5-hydroxypyrazolo[1,5-*a*]quinoxalin-4-ones (**5**) intermediates. This approach was previously followed for the conversion of 1-hydroxyindoles to corresponding NH-indoles [25,26]. As a result of these studies, compounds **4d**–**f** were obtained with this two-stage procedure in yields of up to 79% (method B). The two-stage approach, which proceeded via an *N*-dehydroxylation step, proved to be comparable in terms of yields to the one-step method, which involved hydrogen reduction of *N*-arylpyrazolecarboxylates in the presence of palladium. The two-stage approach can also be applied to the synthesis of a wider range of NH-pyrazolo[1,5-*a*]quinoxalines. This method proved to be particularly useful for obtaining compounds **4d**–**f**.

Substituted 5-hydroxypyrazolo[1,5-*a*]quinoxalin-4-ones **5** were converted in good yields to the stable esters **6a**–**c** in the presence of TEA with bromoacetic acid ethyl ester (Fig. 3).

We performed acetylation of amino-substituted pyrazolo[1,5-*a*]quinoxalin-4-ones (**4**) and 5-hydroxypyrazolo[1,5-*a*]quinoxalines (**5**) with acetic anhydride. The 5-hydroxypyrazolo[1,5-*a*]quinoxaline derivatives **5** were converted to the diacetylated compounds (**7a**–**c**), which readily hydrolyzed in the presence of piperidine (or aqueous K_2CO_3) as base. This method makes it possible to selectively produce monoacetylated products **8a**–**b** (Fig. 4). In contrast, under the same conditions, pyrazolo[1,5-*a*]quinoxalin-4-one derivatives **4** are acetylated only at the substituted amino group (Fig. 5).

The structures of all synthesized compounds **4**–**9** were characterized by a combination of IR and NMR spectroscopy, and mass spectrometry. The structure of compound **5e** was also confirmed by X-ray crystallography (Fig. 6).

2.2. Monoamine oxidase inhibition

The pyrazolo[1,5-*a*]quinoxalin-4-ones were evaluated as potential MAO inhibitors by employing the literature protocol [27,28]. The

Table 1
The human MAO inhibition potencies of pyrazolo[1,5-*a*]quinoxalin-4-ones and related derivatives.

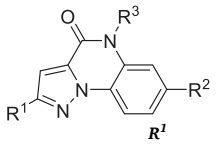

	R^1	R^2	R^3	IC_{50}(μM)[a] MAO-A	MAO-B	SI[b]
4a		COOEt	H	5.51 ± 1.25	>100[c]	>18
4b	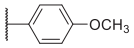	COOEt	H	3.92 ± 0.337	ND[d]	–
4c	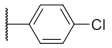	COOEt	H	2.04 ± 0.037	ND[d]	–
4d		CN	H	1.31 ± 0.031	1.28 ± 0.013	0.98
4e	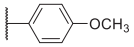	CN	H	>100[c]	0.763 ± 0.035	<0.008
4f	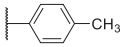	CN	H	5.10 ± 0.131	0.617 ± 0.044	0.12
5a	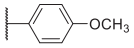	COOEt	OH	22.0 ± 0.750	4.32 ± 0.768	0.20
5b		CN	OH	14.9 ± 0.156	20.8 ± 3.15	1.4
5c	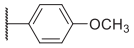	CN	OH	17.0 ± 0.014	4.33 ± 0.018	0.25
5d	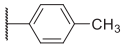	CN	OH	13.4 ± 1.39	4.99 ± 0.663	0.37
5e	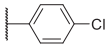	CN	OH	1.83 ± 0.011	>100[c]	>55
5f	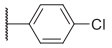	NH_2	OH	0.345 ± 0.0057	>100[c]	>290
6a	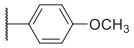	COOEt	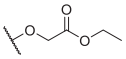	4.36 ± 0.135	>100[c]	>23
6b	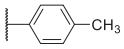	COOEt	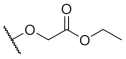	7.65 ± 0.127	>100[c]	>13
6c	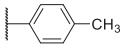	CN	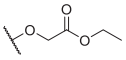	10.9 ± 8.10	0.674 ± 0.003	0.062
7a				0.181 ± 0.0079	>100[c]	>552
7b	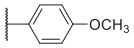			0.155 ± 0.0051	11.9 ± 0.827	77
7c	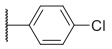			0.028 ± 0.0039	1.40 ± 0.087	50
8a			OH	0.146 ± 0.020	64.4 ± 11.5	441
8b	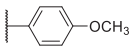		OH	0.472 ± 0.293	7.90 ± 0.470	17
9a			H	0.173 ± 0.010	4.16 ± 0.887	24
9b	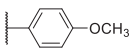		H	0.951 ± 0.087	7.37 ± 1.78	7.7
Curcumin (reference inhibitor)				5.02 ± 0.45	2.56 ± 0.21	0.51

[a] All IC_{50} values are expressed as the mean ± SD of triplicate determinations.
[b] The selectivity index indicates the specificity of inhibition of the MAO-A isoform: SI = IC_{50}(MAO-B)/IC_{50}(MAO-A).
[c] NI - No inhibition at a maximal tested concentration of 100 μM.
[d] ND - IC_{50} not determined due to fluorescence of the inhibitors under the specific assay conditions.

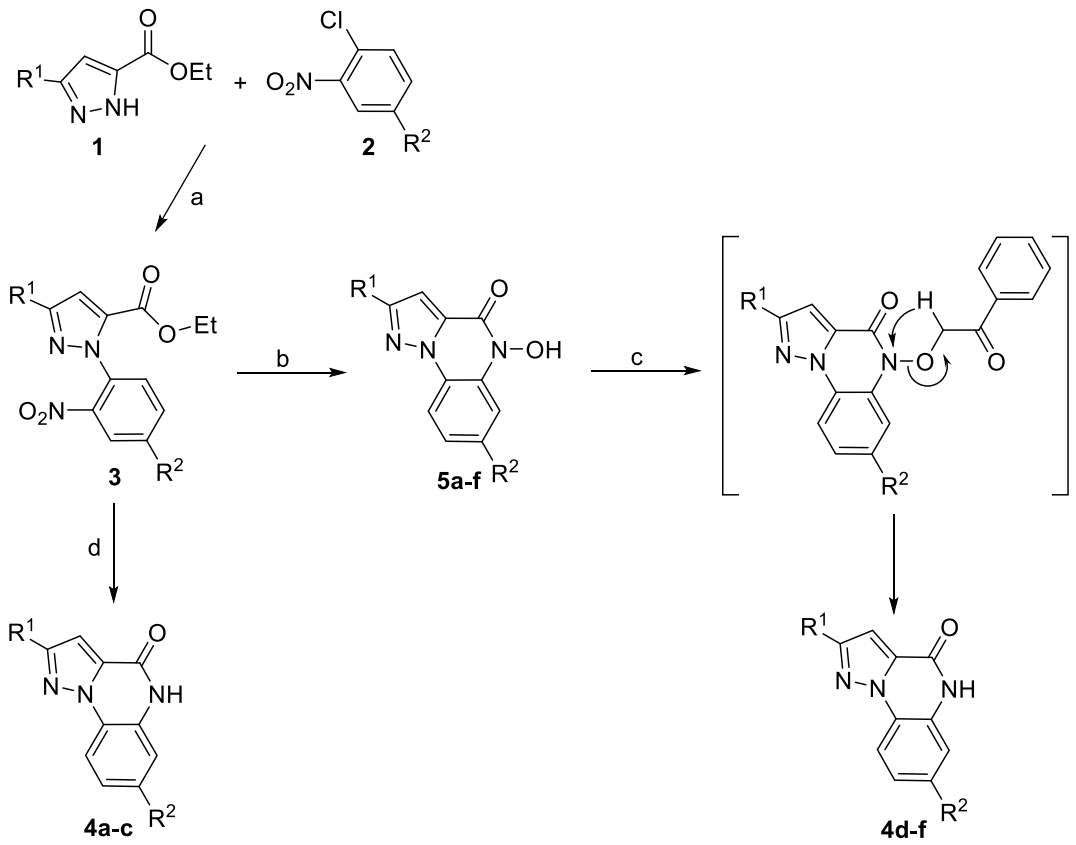

Fig. 2. The synthesis of the pyrazolo[1,5-*a*]quinoxalines **4** and **5**. Key: (a) K_2CO_3, DMF; (b) $SnCl_2$/HCl; (c) phenacyl bromide, TEA, ethanol (method B); (d) methanol, Pd/C (10%), H_2 (4–5 atm), 71–73 °C (method A).

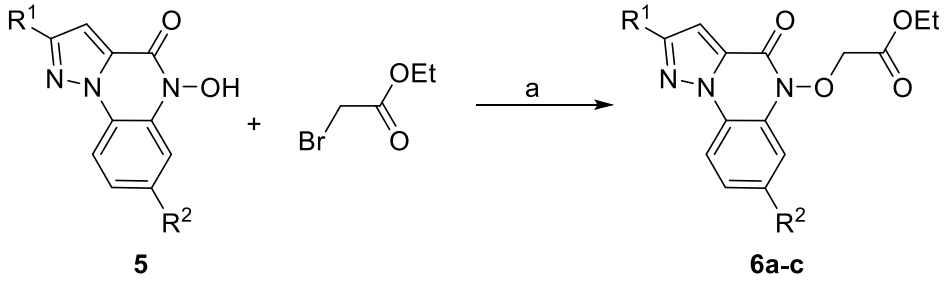

Fig. 3. The synthesis of pyrazolo[1,5-*a*]quinoxaline derivatives **6a**–**c**. Key: (a) TEA, ethanol.

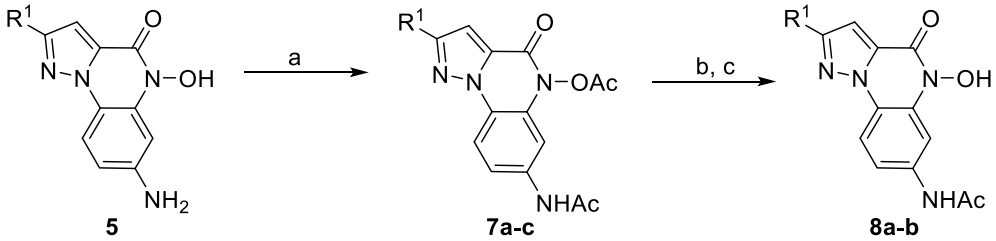

Fig. 4. The synthesis of the acetylated pyrazolo[1,5-*a*]quinoxalines **7** and **8**. Key: (a) Ac_2O/Py, 100 °C; (b) piperidine, ethanol; (c) AcOH.

recombinant human MAOs (Sigma-Aldrich) served as enzyme sources and kynuramine was used as substrate for both enzymes. Kynuramine was used at a concentration of 50 μM, while MAO-A and MAO-B were used at concentrations of 0.0075 and 0.015 mg protein/mL, respectively. The determination of MAO catalytic activity relied on the measurement of formation of 4-hydroxyquinoline, the ultimate product of the MAO-catalyzed oxidation of kynuramine. 4-Hydroxyquinoline was quantitated by fluorescence spectrophotometry (λ_{ex} = 310 nm; λ_{em} = 400 nm) at endpoint after termination of the enzyme reactions with the addition of sodium hydroxide. By measuring the rates of kynuramine oxidation in the presence of a series of test inhibitors (0.003–100 μM), sigmoidal plots of rate versus inhibitor concentration (log[I]) were constructed from which IC_{50} values were determined (Fig. 7).

The IC_{50} values for the inhibition of MAO-A and MAO-B are given in

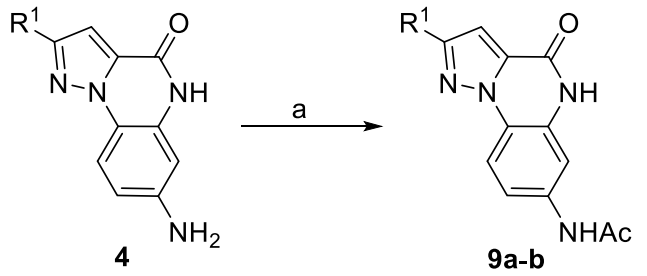

Fig. 5. The synthesis of the acetylated pyrazolo[1,5-*a*]quinoxalines **9a**–**b**. Key: (a) Ac_2O/Py, 100 °C.

table 1, and show that the pyrazolo[1,5-*a*]quinoxalin-4-ones inhibit both MAO isoforms with differing specificities. Among the 22 compounds tested, 8 derivatives inhibit MAO-A with IC_{50} values in the submicromolar range (<1 μM). It is noteworthy that all acetylated derivatives **7**–**9** exhibit submicromolar MAO-A inhibition, with **7c** (IC_{50} = 0.028 μM) being the most potent MAO-A inhibitor of the series. In fact only one compound (**5f**), the amine substituted derivative, among the non-acetylated derivatives (**4**–**6**) possesses an $IC_{50} < 1$ μM. It may thus be concluded that substitution of R^2 with an amine (**5f**) or an acetylated amine (**7**–**9**) yields good potency MAO-A inhibition. No other substituent on R^2 (COOEt, CN) yielded compounds with submicromolar MAO-A inhibition potencies. Although the most potent compound of the series (**7c**) is a diacetylated derivative, no clear trend is established whether monoacetylated or diacetylated compounds are higher potency MAO-A inhibitors (e.g. compare **7a**, **8a**, **9a**, and **7b**, **8b**, **9b**). Another interesting structure–activity relationship (SAR) is that chlorophenyl substitution of R^1 yields higher potency MAO-A inhibition than the other substituents considered (phenyl, anisyl, tolyl) (e.g. compare **4c** vs. **4a**, **4b**; **5e** vs. **5b**–**d**; **7c** vs. **7a**, **7b**). For MAO-A inhibition other clear SAR trends are not observable, although for some derivatives CN substitution on R^2 yields higher potency compared to COOEt substitution (e.g. **4d** vs. **4a**), while some R^3 unsubstituted compounds are higher potency MAO-A inhibitors than the OH substituted homologues (e.g. **4d** vs. **5b**; **4b** vs. **5a**; **4f** vs. **5d**).

For MAO-B inhibition only 3 compounds exhibited $IC_{50} < 1$ μM, with the IC_{50} values ranging from 0.617 to 0.763 μM. Among the SARs that are apparent for MAO inhibition is that CN substitution on R^2 yields higher potency MAO-B inhibition compared to COOEt substitution (e.g. **4d** vs. **4a**; **4e** vs. **4b**; **6c** vs. **6b**). With the exception of **5a** (vs. **4b**), the R^3 unsubstituted compounds are more optimal for MAO-B inhibition to the OH substituted derivatives (e.g. **4d**–**f** vs. **5b**–**d**). It is also noteworthy that the diacetylated compound **7c** is a good potency MAO-B inhibitor while the unacetylated homologue **5f** is not an inhibitor, even at a maximal tested concentration of 100 μM. Although other clear trends are not apparent it may be noted that among the 4 monacetylated compounds (**8**–**9**), 3 exhibit $IC_{50} < 10$ μM, which further support the observation that acetylation is beneficial for MAO-B inhibition. Diacetylated derivative **7c** (IC_{50} = 1.40 μM) and ester **6c** (IC_{50} = 0.674 μM) may also be highlighted as a good potency MAO-B inhibitors.

When specificity of MAO inhibition is considered, compounds **7a** (IC_{50} = 0.181 μM) and **4e** (IC_{50} = 0.763 μM) may be highlighted as good potency and specific inhibitors of the MAO-A and MAO-B isoform,

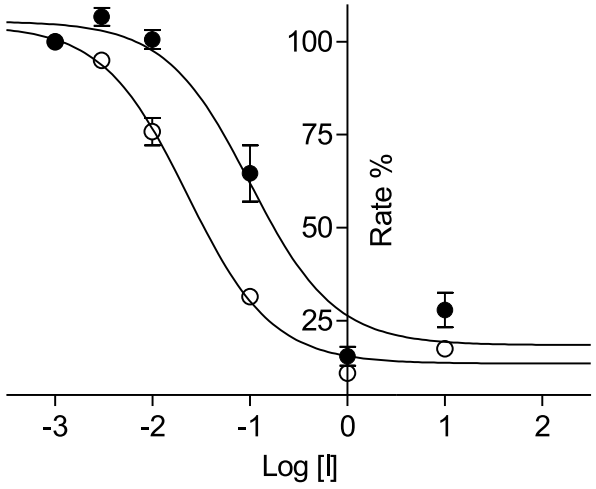

Fig. 7. Sigmoidal dose–response curves for the inhibition of MAO-A by compounds **7c** (open circles) and **8a** (filled circles).

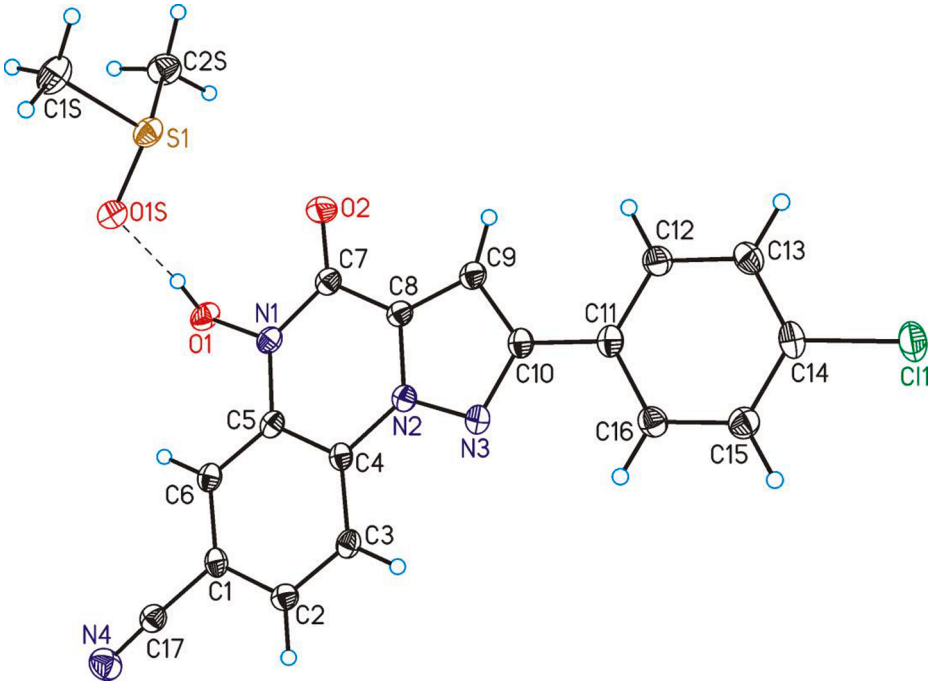

Fig. 6. The X-ray crystal structure of compound **5e** with the atoms represented by thermal displacements ellipsoids with 50% probability.

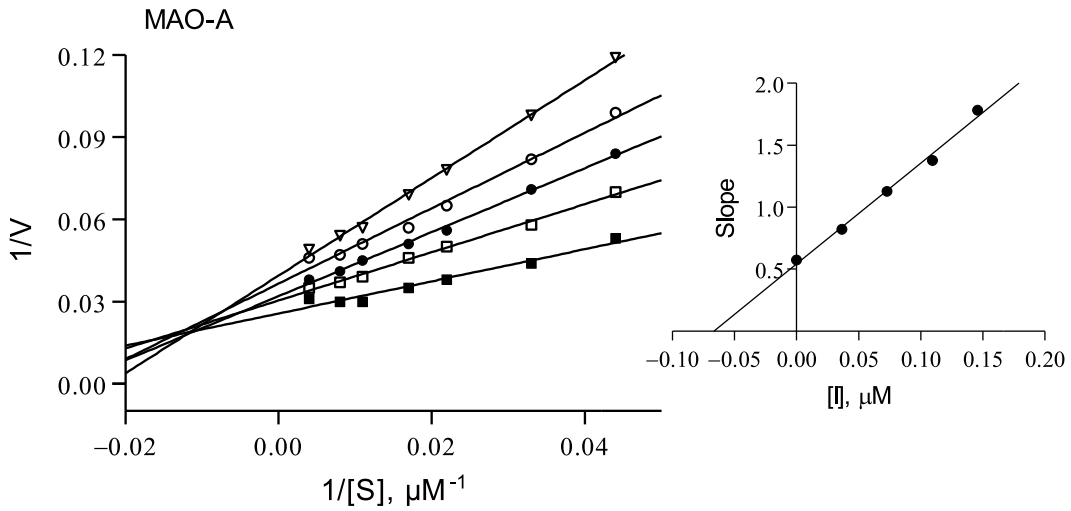

Fig. 8. Lineweaver-Burk plots of MAO-A catalytic activities in the absence (filled squares) and presence of compound **8a**. The inset shows a graph of the slopes of the Lineweaver-Burk plots versus inhibitor concentration.

respectively.

This study highlights several high potency and specific MAO-A inhibitors among the pyrazolo[1,5-*a*]quinoxalin-4-one derivatives. The mode of inhibition of MAO-A (e.g. competitive inhibition) was further investigated for a representative inhibitor, compound **8a**. For this purpose, a set of Lineweaver-Burk plots for the inhibition of MAO-A by compound **8a** was constructed. One plot was constructed in the absence of inhibitor, and four plots were constructed in the presence of the following inhibitor concentrations: ¼ × IC_{50}, ½ × IC_{50}, ¾ × IC_{50} and 1 × IC_{50} (Fig. 8). For each plot, the kynuramine concentration ranged from 22.5 to 250 μM. The Lineweaver-Burk plots constructed were found to be linear and are indicative that the inhibitor acts as a competitive MAO-A inhibitor. From the Lineweaver-Burk plots, a K_i value of 0.067 μM was estimated for the inhibition of MAO-A by this inhibitor.

2.3. Molecular modeling

To gain insight into binding modes and interactions of selected pyrazolo[1,5-*a*]quinoxalin-4-ones in the active sites of MAO-A and MAO-B, molecular docking experiments were carried out with the Discovery Studio 3.1 suite of software (Accelrys) using the CDOCKER application as described previously [28]. As protein models, X-ray crystal structures of human MAO-A co-crystallised with harmine (PDB entry: 2Z5X) and human MAO-B co-crystallised with safinamide (PDB entry: 2V5Z) were obtained from the protein data bank [6,29].

As mentioned, compounds with tricyclic fused ring systems such as harmine potently inhibit MAO-A [6]. It is therefore not surprising that a number of the pyrazolo[1,5-*a*]quinoxalin-4-ones of this study are high potency MAO-A inhibitors. Molecular docking with **5f** shows that this compound fits within the MAO-A active site and is orientated with the amine group directed towards the FAD, where it is within hydrogen bond distance from two conserved active site waters (Fig. 9). Interestingly, the *N*-OH is hydrogen bonded to N5 of the FAD. The chlorine is directed towards the entrance of the active site and may form a halogen bond with Ala-111. Pi-interactions between the aromatic rings of the inhibitor and Phe-208, Phe-352 and Tyr-407 are also possible. Larger pyrazolo[1,5-*a*]quinoxalin-4-one inhibitors such as the diacetylated compound **7c**, does not fit within the MAO-A active site, even though it is the most potent inhibitor of the series. This result suggests that induced fit and likely the displacement of conserved water molecules must occur for **7c** to bind, which may, at least in part, explain the high affinity of this compound for MAO-A. To investigate this, the structure of **7c** was superimposed on the docked orientation of **5f**, and the resulting pose was refined using in situ minimization allowing for flexibility of the active site residues. Interestingly, for **7c** hydrogen bonding may occur with Tyr-197 at the bottom of the active site while pi-interactions occur between the aromatic rings of the inhibitor and Phe-208, Phe-352 and Tyr-444. Unfavourable steric interactions may be possible between the chlorine substituent of the inhibitor and Leu-97 and Ile-325, and between the phenyl substituent and Cys-323. It may be speculated that some degree of flexibility of these residues as well as the displacement of two conserved water molecules will be required when **7c** binds to MAO-A.

Docking of the good potency MAO-B inhibitor, **4e**, into MAO-B shows that the tricyclic ring system binds within the substrate cavity with the methoxyphenyl ring extending into the entrance cavity beyond Ile-199. Although no hydrogen bonding occurs, the inhibitor is stabilized by pi-pi interactions between the aromatic rings of the inhibitor and Tyr-326 and pi-sulfur interactions with Cys-172. The inhibitor is thus mainly stabilized by van der Waals interactions in MAO-B.

3. Conclusion

In conclusion, the present study discovers a number of pyrazolo[1,5-*a*]quinoxalin-4-one derivatives that are good potency inhibitors of human MAO-A and MAO-B. Among the studied compounds, 8 derivatives inhibit MAO-A with $IC_{50} < 1$ μM. Interestingly, the most potent MAO-A inhibitor, **7c** ($IC_{50} = 0.028$ μM), does not fit within the MAO-A active site as evaluated by molecular docking experiments. This result suggests that induced fit and likely the displacement of conserved water molecules must occur for **7c** to bind, and may explain the high affinity of this compound for MAO-A. Among the studied compounds, 3 derivatives inhibit MAO-B with $IC_{50} < 1$ μM, with the most potent inhibitor (**4f**) possessing an IC_{50} value of 0.617 μM. Derivatives that display specific inhibition of an MAO isoform were discovered, with particularly **7a** ($IC_{50} = 0.181$ μM) and **4e** ($IC_{50} = 0.763$ μM) being good potency and specific inhibitors of MAO-A and MAO-B, respectively. This is the first report of MAO inhibition by pyrazolo[1,5-*a*]quinoxalin-4-one derivatives, and this study concludes that these compounds are suitable leads for the future development of MAO inhibitors, particularly of the MAO-A isoform.

It is important to consider whether these compounds would be absorbed from the gastrointestinal tract and gain access to the central nervous system. To examine this possibility, physicochemical properties were calculated and interpreted with the SwissADME tool, provided by the Swiss Institute of Informatics [31]. The SwissADME tool predicts brain penetration and oral bioavailability by calculating key physiochemical properties such as molecular weight, lipophilicity, polarity,

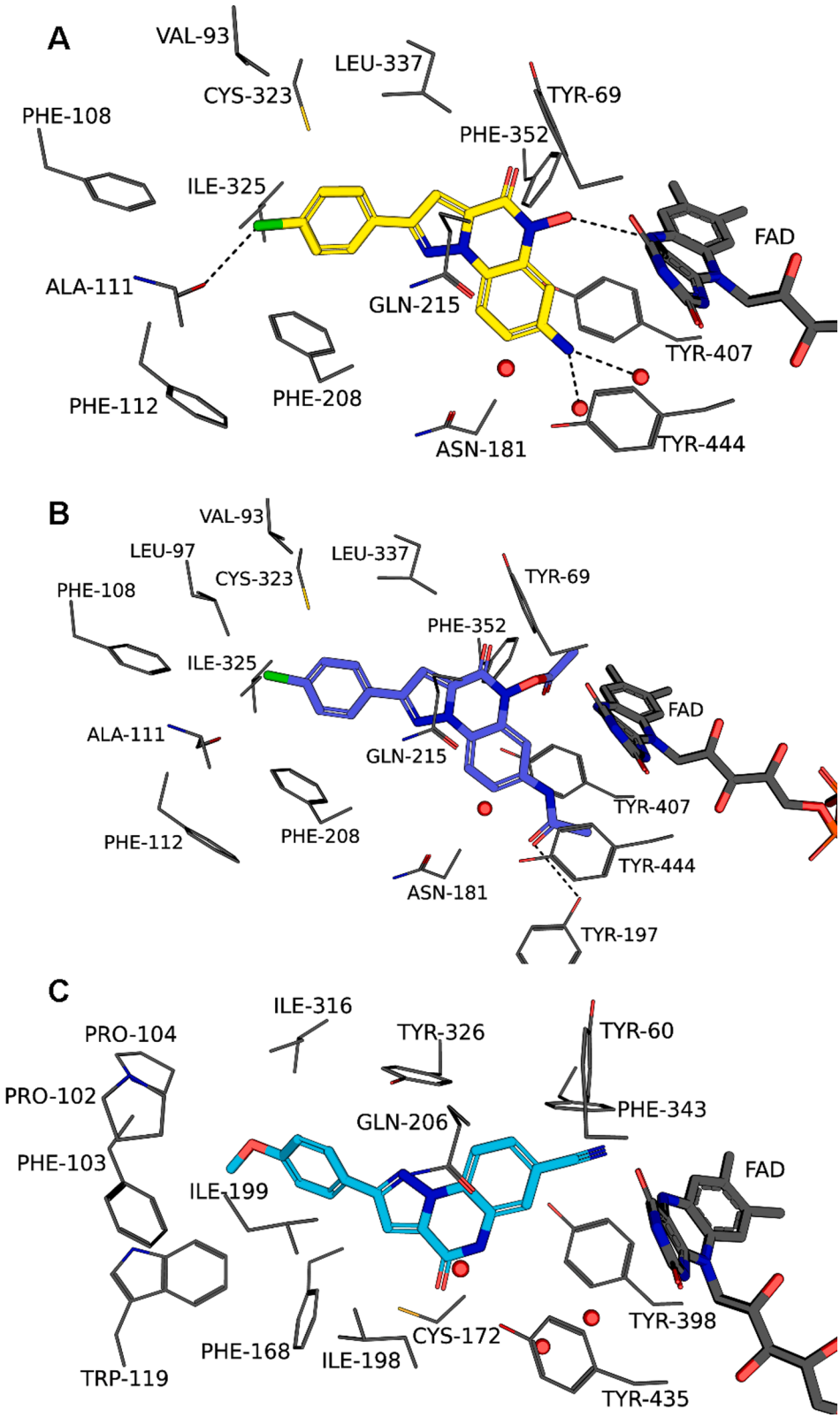

Fig. 9. The predicted binding orientations of **5f** (A) and **7c** (B) to MAO-A, and **4e** to MAO-B (C). Illustrations were prepared with the PyMOL molecular graphics system [30].

solubility, flexibility, saturation, molecular refractivity and polar surface area (tPSA). The compounds of this study show high *in silico* gastrointestinal absorption, while most compounds are predicted not possess brain penetration (Table S1, supplementary material), primarily because of high tPSA (>80 Å^2). Among the compounds (**4a**, **4c**, **4d**, **4f**) that do exhibit *in silico* brain penetration is **4f**, the most potent MAO-B inhibitor of the study. This underscores the potential of this compound as a possible centrally active MAO-B inhibitor. These data also show that future structure modification of the pyrazolo[1,5-*a*]quinoxalin-4-ones should aim to reduce polarity and tPSA.

Declaration of Competing Interest

The authors declared that there is no conflict of interest.

Acknowledgements

This work was financially supported by the National Research Foundation of South Africa [Grant specific unique reference numbers (UID) 85642 and 96180]. The Grantholders acknowledge that opinions, findings and conclusions or recommendations expressed in any publication generated by the NRF supported research are that of the authors, and that the NRF accepts no liability whatsoever in this regard. The X-ray diffraction experiment was carried out using equipment from the Center for Molecular Structure Studies at A.N. Nesmeyanov Institute of Organoelement Compounds operating with financial support of the Ministry of Science and Higher Education of the Russian Federation.

Appendix A. Supplementary data

Supplementary data to this article can be found online at https://doi.org/10.1016/j.bioorg.2020.104563.

References

[1] M.B. Youdim, Y.S. Bakhle, Monoamine oxidase: isoforms and inhibitors in Parkinson's disease and depressive illness, Br. J. Pharmacol. 147 (Suppl 1) (2006) S287–S296, https://doi.org/10.1038/sj.bjp.0706464.
[2] J.C. Shih, K. Chen, M.J. Ridd, MONOAMINE OXIDASE: From Genes to Behavior, Annu. Rev. Neurosci. 22 (1) (1999) 197–217.
[3] J.C. Shih, Monoamine oxidase isoenzymes: genes, functions and targets for behavior and cancer therapy, J. Neural Transm. 125 (11) (2018) 1553–1566, https://doi.org/10.1007/s00702-018-1927-8.
[4] L.W. Thorpe, K.N. Westlund, L.M. Kochersperger, C.W. Abell, R.M. Denney, Immunocytochemical localization of monoamine oxidases A and B in human peripheral tissues and brain. J. Histochem. Cytochem. 35 (1) (1987) 23–32.
[5] M.J. Rodríguez, J. Saura, E.E. Billett, C.C. Finch, N. Mahy, Cellular localization of monoamine oxidase A and B in human tissues outside of the central nervous system, Cell Tissue Res. 304 (2) (2001) 215–220, https://doi.org/10.1007/s004410100361.
[6] S.-Y. Son, J. Ma, Y. Kondou, M. Yoshimura, E. Yamashita, T. Tsukihara, Structure of human monoamine oxidase A at 2.2-A resolution: The control of opening the entry for substrates/inhibitors, Proc. Natl. Acad. Sci. 105 (15) (2008) 5739–5744.
[7] C. Binda, P. Newton-Vinson, F. Hubalek, D.E. Edmondson, A. Mattevi, Structure of human monoamine oxidase B, a drug target for the treatment of neurological disorders, Nat. Struct. Biol. 9 (1) (2002) 22–26, https://doi.org/10.1038/nsb732.
[8] M.B.H. Youdim, D. Edmondson, K.F. Tipton, The therapeutic potential of monoamine oxidase inhibitors, Nat. Rev. Neurosci. 7 (4) (2006) 295–309.
[9] R.R. Ramsay, Molecular aspects of monoamine oxidase B, Prog. Neuro-Psychopharmacol. Biol. Psychiatry 69 (2016) 81–89.
[10] S. Gaur, M.E. Gross, C.-P. Liao, B. Qian, J.C. Shih, Effect of Monoamine oxidase A (MAOA) inhibitors on androgen-sensitive and castration-resistant prostate cancer cells, Prostate 79 (6) (2019) 667–677.
[11] S. Deshwal, M. Di Sante, F. Di Lisa, N. Kaludercic, Emerging role of monoamine oxidase as a therapeutic target for cardiovascular disease, Curr. Opin. Pharmacol. 33 (2017) 64–69.
[12] S. Carradori, D. Secci, J.P. Petzer, MAO inhibitors and their wider applications: a patent review, Expert Opin. Ther. Pat. 28 (3) (2018) 211–226.
[13] M. Naoi, W. Maruyama, M. Shamoto-Nagai, Type A monoamine oxidase and serotonin are coordinately involved in depressive disorders: from neurotransmitter imbalance to impaired neurogenesis, J. Neural Transm. 125 (1) (2018) 53–66, https://doi.org/10.1007/s00702-017-1709-8.
[14] T. Müller, Pharmacokinetics and pharmacodynamics of levodopa/carbidopa cotherapies for Parkinson's disease, Expert Opin. Drug Metab. Toxicol. 16 (5) (2020) 403–414.
[15] J. Lieb, Remission of rheumatoid arthritis and other disorders of immunity in patients taking monoamine oxidase inhibitors, Int. J. Immunopharmacol. 5 (4) (1983) 353–357.
[16] R.E. Kast, Crohn's disease remission with phenelzine treatment, Gastroenterology 115 (4) (1998) 1034–1035.
[17] D.E. Edmondson, Hydrogen peroxide produced by mitochondrial monoamine oxidase catalysis: biological implications, Curr. Pharm. Des. 20 (2) (2014) 155–160, https://doi.org/10.2174/13816128113190990406.
[18] J. Mialet-Perez, Y. Santin, A. Parini, Monoamine oxidase-A, serotonin and norepinephrine: synergistic players in cardiac physiology and pathology, J. Neural Transm. 125 (11) (2018) 1627–1634, https://doi.org/10.1007/s00702-018-1908-y.
[19] N. Kaludercic, J. Mialet-Perez, N. Paolocci, A. Parini, F. Di Lisa, Monoamine oxidases as sources of oxidants in the heart, J. Mol. Cell. Cardiol. 73 (2014) 34–42.
[20] R.R. Ramsay, A. Albreht, Kinetics, mechanism, and inhibition of monoamine oxidase, J. Neural Transm. 125 (11) (2018) 1659–1683.
[21] V.A. Panova, M.K. Korsakov, A.A. Shetnev, S.I. Filimonov, Synthesis of substituted 5-hydroxypyrazolo[1,5-a]quinoxalin-4-ones, Mendeleev Commun. 29 (1) (2019) 114–115.
[22] Kant BR, Kant BS, Chand BT, Kumar BA. Green synthesis of hydroxamic acid and its potential industrial applications. In: Kalia VC, ed. Microbial Applications Vol.2: Biomedicine, Agriculture and Industry. Springer International Publishing; 2017: 169-184.
[23] T. Ikawa, Y. Fujita, T. Mizusaki, S. Betsuin, H. Takamatsu, T. Maegawa, Y. Monguchi, H. Sajiki, Selective N-alkylation of amines using nitriles under hydrogenation conditions: facile synthesis of secondary and tertiary amines, Org. Biomol. Chem. 10 (2) (2012) 293–304.
[24] S. Maki, M. Okawa, T. Makii, T. Hirano, H. Niwa, Pd black deposited on polypropylene sheet as a highly selective catalyst for hydrogenation of alkenes, Tetrahedron Lett. 44 (18) (2003) 3717–3721.
[25] Z.V. Chirkova, M.V. Kabanova, S.I. Filimonov, I.G. Abramov, A. Petzer, I. Engelbrecht, J.P. Petzer, K. Yu Suponitsky, A.V. Veselovsky, An investigation of the monoamine oxidase inhibition properties of pyrrolo[3,4- f]indole-5,7-dione and indole-5,6-dicarbonitrile derivatives, Drug Dev. Res. 79 (2) (2018) 81–93.
[26] Z.V. Chirkova, M.V. Kabanova, S.I. Filimonov, E.A. Smirnova, General synthetic method for NH-indoles starting from N-hydroxyindoles, Russ. Chem. Bull. 68 (6) (2019) 1196–1199.
[27] L. Novaroli, M. Reist, E. Favre, A. Carotti, M. Catto, P.-A. Carrupt, Human recombinant monoamine oxidase B as reliable and efficient enzyme source for inhibitor screening, Bioorg. Med. Chem. 13 (22) (2005) 6212–6217.
[28] S. Mostert, A. Petzer, J.P. Petzer, Indanones As High-Potency Reversible Inhibitors of Monoamine Oxidase, ChemMedChem 10 (5) (2015) 862–873.
[29] C. Binda, J. Wang, L. Pisani, C. Caccia, A. Carotti, P. Salvati, D.E. Edmondson, A. Mattevi, Structures of human monoamine oxidase B complexes with selective noncovalent inhibitors: safinamide and coumarin analogs, J. Med. Chem. 50 (23) (2007) 5848–5852, https://doi.org/10.1021/jm070677y.
[30] W.L. DeLano, The PyMOL molecular graphics system, DeLano Scientific, San Carlos, USA, 2002.
[31] A. Daina, O. Michielin, V. Zoete, SwissADME: a free web tool to evaluate pharmacokinetics, drug-likeness and medicinal chemistry friendliness of small molecules, Sci. Rep. 7 (1) (2017), https://doi.org/10.1038/srep42717.